Applied Physics Letters

Dirac energy spectrum and inverted bandgap in metamorphic InAsSb/InSb superlattices

Cite as: Appl. Phys. Lett. **116**, 032101 (2020); https://doi.org/10.1063/1.5128634
Submitted: 20 September 2019 . Accepted: 05 December 2019 . Published Online: 21 January 2020

Sergey Suchalkin, Maksim Ermolaev, Tonica Valla, Gela Kipshidze, Dmitry Smirnov, Seongphill Moon, Mykhaylo Ozerov, Zhigang Jiang, Yuxuan Jiang, Stefan P. Svensson, Wendy L. Sarney, and Gregory Belenky

Applied Physics Letters ARTICLE scitation.org/journal/apl

Dirac energy spectrum and inverted bandgap in metamorphic InAsSb/InSb superlattices

Cite as: Appl. Phys. Lett. **116**, 032101 (2020); doi: 10.1063/1.5128634
Submitted: 20 September 2019 · Accepted: 5 December 2019 ·
Published Online: 21 January 2020

Sergey Suchalkin,[1,a)] Maksim Ermolaev,[1] Tonica Valla,[2] Gela Kipshidze,[1] Dmitry Smirnov,[3] Seongphill Moon,[3,4] Mykhaylo Ozerov,[3] Zhigang Jiang,[5] Yuxuan Jiang,[5] Stefan P. Svensson,[6] Wendy L. Sarney,[6] and Gregory Belenky[1]

AFFILIATIONS

[1]Stony Brook University, Electrical and Computer Engineering, Stony Brook, New York 11794, USA
[2]Brookhaven National Laboratory, Upton, New York 11973, USA
[3]National High Magnetic Field Laboratory, Tallahassee, Florida 32310, USA
[4]Department of Physics, Florida State University, Tallahassee, Florida 32306, USA
[5]Georgia Institute of Technology, Atlanta, Georgia 30332, USA
[6]U.S. Army Research Laboratory, 2800 Powder Mill Rd., Adelphi, Maryland 20783, USA

[a)]Electronic mail: Sergey.Suchalkin@stonybrook.edu

ABSTRACT

A Dirac-type energy spectrum was demonstrated in gapless ultrashort-period metamorphic InAsSb/InSb superlattices by angle-resolved photoemission spectroscopy (ARPES) measurements. The Fermi velocity value of 7.4×10^5 m/s in a gapless superlattice with a period of 6.2 nm is in good agreement with the results of magnetoabsorption experiments. An "inverted" bandgap opens in the center of the Brillouin zone at higher temperatures and in the superlattice with a larger period. The ARPES data indicate the presence of a surface electron accumulation layer.

The virtual substrate approach[1] makes it possible to fabricate narrow gap InAsSb-based superlattices (SLs) with ultrathin layers, formed by engineered ordering of the group V element composition.[2] Such structures allow easy bandgap control and tailoring of carrier dispersion.[3] The exceptional design flexibility originates from the large lattice mismatch and broken gap band alignments between the corresponding binaries—InAs and InSb.[4] The electronic and optical properties of $InAs_{1-x}Sb_x/InAs_{1-y}Sb_y$ SLs differ from those of bulk InAsSb alloys. While the minimum bandgap of the random alloy reached at the Sb composition of ~0.6 is ~100 meV,[5–7] the bandgap of an InAsSb/InSb superlattice can be reduced to zero and beyond to negative values by increasing the SL period.[3,8] These engineered semiconductor materials can host nontrivial topological states.[9,10] For example, a new topological semimetal (TSM) phase—a triple point TSM—is predicted in an InAsSb alloy with short-period group V composition ordering along the [111] direction.[10,11] High intrinsic spin–orbit coupling, high carrier mobility, the possibility of magnetic doping, and an ability to form a good interface with a superconductor (Al) make the $InAs_{1-x}Sb_x/InAs_{1-y}Sb_y$ SL a perfect candidate for a new material platform for quantum information devices.

To probe the bandgaps of alloys and SLs down to ~70 meV, photoluminescence can be used. For the nearly gapless SLs, alternative experimental methods for the investigations of the band structure such as infrared magnetoabsorption must be used.[7,12–14] More detailed information can be gained through angle-resolved photoemission spectroscopy (ARPES), which is a direct experimental method to study the band structure and carrier dispersion of materials[15] near the surface. However, the application of this method to many SLs is limited since the ARPES probing depth (few nanometers) is usually shorter than the SL structure period. For example, the semiconductor–semimetal transition in pseudomorphically grown InAs/GaSb SLs on GaSb happens at a period of ~17 nm, and so using ARPES to obtain electron dispersion in such structures might be problematic. The bandgap of our new metamorphically grown InAsSb/InSb SLs becomes 0 at a SL period of 6.2 nm, and ARPES can be used to monitor carrier dispersion near the semiconductor–semimetal transition point.

In this work, we present ARPES studies of nearly gapless short-period InAsSb/InSb metamorphic superlattices. The ARPES setup includes a Scienta R4000-WAL electron spectrometer with a wide acceptance angle (~30°), providing for simultaneous detection

over a wide range of the momentum space with an ∼0.1° precision.[16,17] The photon source is a Scienta VUV5k microwave-driven plasma-discharge lamp with a monochromator, providing a He *I* radiation (21.22 eV). The combined energy resolution used in the present study was 5 meV. A fully motorized 5-axis manipulator is equipped with a Janis flow cryostat that allows cooling the sample down to 6 K. A relatively low resolution with respect to the momentum component k_Z along the SL growth direction resulted in the averaging of the ARPES spectra over the entire range of k_Z values in the SL Brillouin zone.

The structures grown for ARPES are InAsSb/InSb superlattices with periods of 6.2 and 7.8 nm. The structure details are identical to those reported in Ref. 8, except that the ARPES samples were grown without either a top barrier or a cap layer. The SLs used for the ARPES studies were terminated with the ternary layer. The sample surfaces were protected from contamination by low-temperature deposition of a thick As layer in the MBE chamber.

After the MBE growth, the wafers were transported to the ARPES setup in Ar-filled containers and then loaded into the analysis chamber where the protective cap was removed by heating the sample to ∼300 C. The effectiveness of the As cap was checked at both facilities: we exposed a sample to air for 24 h, then placed it back to the MBE chamber, annealed off the cap, and verified that a good reflection high energy electron diffraction pattern could again be observed, while in the ARPES chamber, both the low-energy electron diffraction (LEED) and ARPES indicated a high quality of decapped surfaces.

The ARPES spectra for two temperatures (40 and 300 K) of the SL with a period of 6.2 nm are presented in Fig. 1. Signal intensity is shown in the gray-scale where the darker area corresponds to higher intensity. At low temperature, the in-plane low-energy electronic structure shows an isotropic "hourglass" like dispersion near the zone center [Figs. 1(a)–1(d)] with the conduction and valence bands practically touching, indicating a nearly gapless SL. A limited energy resolution and an intrinsic broadening of the states do not allow us to conclude whether this is a truly gapless SL or a small gap of about a few millielectronvolts is present. The zero gap is obtained from 8 band k∗p calculations, as shown in Fig. 1(d), indicating that this SL is a 3D Dirac semimetal. The calculations were performed using the Nextnano3 software package.[18] When obtaining the material parameters for the ternary layers, we have taken into account the bowing of the bandgap with a bowing parameter of 0.87 eV,[5,6] the bowing of the spin–orbit splitting with a coefficient of 1.3 eV (Ref. 4), and the bowing of the Kane matrix element of 25 eV.[7] The resulting bowing of electron effective mass was $0.04m_0$ and is in good agreement with the one obtained experimentally in Ref. 6. To take into account the interface disorder, which is seen at high resolution TEM images,[8] the sharp interfaces between the SL layers were replaced with 0.3 nm wide layers with a linear grading of the As composition. The distribution of bowing between conduction and valence bands was used as a fitting parameter. The best fit for experimental data was obtained at the conduction band bowing of 0.65 eV and the valence band bowing of 0.22 eV.

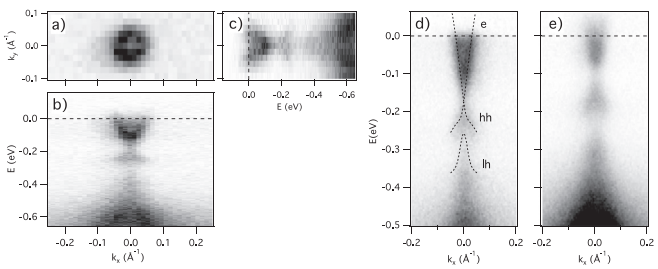

FIG. 1. The electronic structure of $InAs_{0.48}Sb_{0.52}$/InSb SL with a period of 6.2 nm. The Fermi surface (a) and dispersion of the low-energy excitations along the two perpendicular momentum lines [(b) and (c)] indicate an isotropic in-plane electronic structure. The low-temperature electronic structure [(a)–(d)] is nearly gapless. The 300 K spectrum (e) shows a finite gap. Dashed lines in (d) are band-fits based on 8 × 8 k∗p calculations.[18]

The increase in temperature leads to the band energies shifting to higher values and the opening of a sizable gap [Fig. 1(e)], approximately 40 meV. Based on the results of the band structure simulations at 300 K, we attribute the observed bandgap to the hybridization effects where the conduction and valence bands overlap, producing inverted bandgaps, with the SL becoming semimetallic. The effect of high temperature was taken into account by the introduction of experimental temperature coefficients of InSb, InAsSb bandgap, and modification of bandgap-related k∗p parameters.[19]

The Fermi energy extracted from the low-temperature ARPES data is ∼150 meV, roughly 4 times higher than that obtained from the bulk Hall measurements.[20] The most likely reason for this is the presence of a surface accumulation layer.[21–23] The Fermi energy value is in reasonable agreement with estimates based on knowledge of the position of the Fermi-stabilization level and the bending of the conduction band edge energy near the surface. Additionally, nonequilibrium carriers induced by the probe illumination may contribute to an excess band filling. The signal from the SL valence band is weaker than that from the conduction band since the holes are mostly localized in the InSb layers, and the first hole containing the InSb layer is located deeper under the sample surface. The value of the Fermi velocity near the Γ point obtained from an 8 × 8 k∗p model [Fig 1(a)] is 7.4×10^5 m/s.[8] This is somewhat higher than that obtained from our previous ternary–ternary SLs.[3] The difference can be explained by better electron-hole overlap in the InAsSb/InSb SL.

The Dirac character of the carrier dispersion, directly observable in ARPES studies, is also confirmed by the results of the magnetoabsorption measurements (Fig. 2). The square root dependence of the cyclotron resonance transition energy (lines 1 and 2 in Fig. 2) on the magnetic field is a manifestation of the linear dispersion.[24] The gapless character of the SL is established by the zero intercept of the concurrent lines corresponding to the interband transitions.

Based on the calculations, a hybridization gap that appears at 300 K results from the band overlap and anticrossing, and so the SL becomes semimetallic. Characteristic features of the carrier dispersion in the semimetallic SL having cubic crystal symmetry are a gap formed by band anticrossing in the in-plane direction at the zero wave vector component in the growth direction ($k_Z = 0$) and two anisotropic Dirac points due to band crossing at two symmetrical points $\pm k_{Z0} \neq 0$ [Fig. 3(b)].[22,25–27] Such an energy spectrum is, in general, similar to that predicted in InAsSb alloys with CuPt type ordering.[10] In our case, the growth direction is [001], and so the SL has the symmetry of an InAsSb alloy with the CuAu type of ordering.[28] Taking into account the lack of the inversion symmetry in zinc blend crystals and the fact that the order of the [001] symmetry axis (S_4) is different from that of

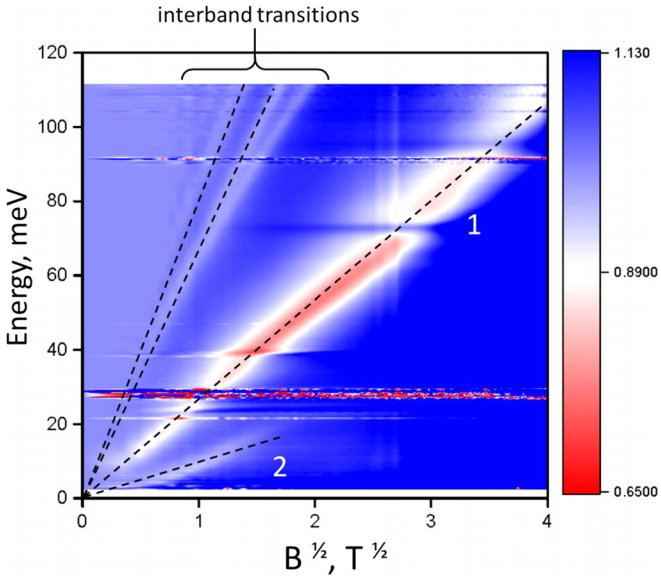

FIG. 2. Color plot of the absorption as a function of the emission energy and square root of the magnetic field. Line 1 corresponds to the transition between the 0th and the 1st electron Landau level and line 2 to the transition between the 1st and the 2nd electron Landau level. The dashed lines are guides to the eye.

[111] (C_3), we can expect that the "fine structure" of the crossing points in our case will be different from that described in Ref. 10. The detailed analysis of the band degeneracies at the crossing points will be given elsewhere. The presence of the SL growth axis reduces the Td symmetry of the bulk zinc blende material thus allowing electron spin splitting, proportional to the wave vector k (Rashba splitting).[29] This makes the SL a new material for realization a "triple point" topological semimetal phase.[10]

The transition in the electronic structure with temperature observed here for a nearly gapless SL is likely the first example of a material that changes its character from a trivial to topological semimetal with a relatively small change in temperature. We expect that a moderate pressure could induce a similar transition for a nearly gapless SL.

An increase in the SL period leads to overlap between the conduction and valence bands of the SL. The ARPES spectrum of the SL with a period of 7.8 nm is presented in Fig. 3(a). In contrast to Fig. 2(a), a finite gap of approximately 30 meV separating upper and lower parts of the hourglasslike pattern is clearly seen. There is a residual signal in the gap, however, which can be a signature of the band crossings taking place at two symmetrical points with zero $k_{x,y}$ and nonzero $\pm k_{Z0} \neq 0$. The ARPES spectra represent the effective average over different values of k_Z within the SL Brillouin zone. The ARPES probing depth is mainly determined by the electron inelastic mean free path, which is in the nanometer range for the probing emission quantum energy of 21 eV.[30] At these conditions, the presented ARPES image is the result of averaging over the whole SL Brillouin zone. Therefore, even in the case of the bandgap opening near $k_Z = 0$, we can expect to see some signal contribution from two Dirac points at some $\pm k_{Z0} \neq 0$.

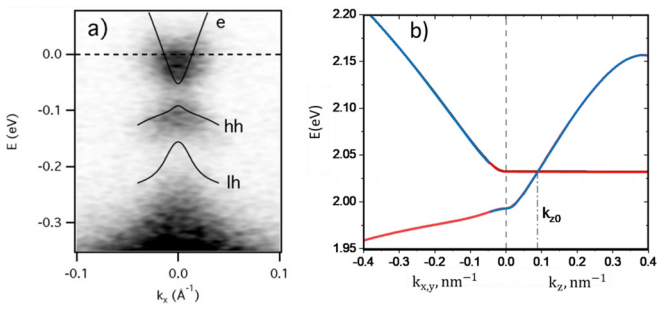

FIG. 3. (a) ARPES spectrum of the InAsSb/InSb SL with a period of 7.8 nm, recorded at T = 108 K. The solid lines represent the 8-band k∗p calculations. (b) Calculated carrier dispersion of the band-inverted SL for $k_{x,y}$ and k_Z. The blue curve indicates electronlike states, while the red curve indicates the holelike ones.

The low intensity of this signal can be caused by the strong reduction of the density of states as k_Z approaches the middle of the SL Brillouin zone.

In conclusion, we have presented measurements of the carrier dispersion in short-period metamorphic InAsSb/InSb ultranarrow gap superlattices. The Dirac character of the dispersion with a Fermi velocity of 7.4×10^5 m/s in the gapless SL was demonstrated. The energy gap at $k_Z = 0$ changes from 0 to an inverted one of 30 meV as the SL period is increased from 6.2 to 7.8 nm. The data demonstrate that the character of the energy dispersion in a short-period metamorphic InAsSb/InSb SL is similar to the type of dispersion in the corresponding bulk alloys with compositional ordering. In contrast to the latter, the SL energy spectrum can be predicted by and controlled with the structure's design. This control makes metamorphic InAsSb/InSb SLs a flexible platform for realizing quantum materials and developing a variety of optoelectronic and quantum devices.

The work of M.E., S.S., G.B., and G.K. was supported by the National Science Foundation under Grant No. DMR-1809708, the U.S. Army Research Office under Grant No. W911TA-16-2-0053, and by the Center of Semiconductor Materials and Device Modeling. The work of Z.J. was supported by the NSF under Grant No. DMR-1809120. ARPES experiments at the Brookhaven National Laboratory were supported by the U.S. Department of Energy, Office of Basic Energy Sciences, Contract No. DE-SC0012704. S.M. and D.S. acknowledge the support from the U.S. Department of Energy (Grant No. DE-FG02-07ER46451) for IR magnetospectroscopy measurements that were performed at the National High Magnetic Field Laboratory, which was supported by the National Science Foundation (NSF) under Cooperative Agreement Nos. DMR-1157490 and DMR-1644779, and the State of Florida.

REFERENCES

[1]G. Belenky, D. Donetsky, G. Kipshidze, D. Wang, L. Shterengas, W. L. Sarney, and S. P. Svensson, Appl. Phys. Lett. **99**(14), 141116 (2011).
[2]G. Belenky, Y. Lin, L. Shterengas, D. Donetsky, G. Kipshidze, and S. Suchalkin, Electron. Lett. **51**(19), 1521 (2015).
[3]S. Suchalkin, G. Belenky, M. Ermolaev, S. Moon, Y. X. Jiang, D. Graf, D. Smimov, B. Laikhtman, L. Shterengas, G. Kipshidze, S. P. Svensson, and W. L. Sarney, Nano Lett. **18**(1), 412 (2018).
[4]I. Vurgaftman, J. R. Meyer, and L. R. Ram-Mohan, J. Appl. Phys. **89**(11), 5815 (2001).

[5]S. P. Svensson, W. L. Sarney, H. Hier, Y. Lin, D. Wang, D. Donetsky, L. Shterengas, G. Kipshidze, and G. Belenky, Phys. Rev. B **86**(24), 245205 (2012).
[6]S. Suchalkin, J. Ludwig, G. Belenky, B. Laikhtman, G. Kipshidze, Y. Lin, L. Shterengas, D. Smirnov, S. Luryi, W. L. Sarney, and S. P. Svensson, J. Phys. D: Appl. Phys. **49**(10), 105101 (2016).
[7]S. N. Smith, C. C. Phillips, R. H. Thomas, R. A. Stradling, I. T. Ferguson, A. G. Norman, B. N. Murdin, and C. R. Pidgeon, Semicond. Sci. Technol. **7**(7), 900 (1992).
[8]M. Ermolaev, S. Suchalkin, G. Belenky, G. Kipshidze, B. Laikhtman, S. Moon, M. Ozerov, D. Smirnov, S. P. Svensson, and W. L. Sarney, Appl. Phys. Lett. **113**(21), 213104 (2018).
[9]S. Namjoo, A. S. H. Rozatian, and I. Jabbari, J. Alloys Compd. **628**, 458 (2015).
[10]G. W. Winkler, Q. S. Wu, M. Troyer, P. Krogstrup, and A. A. Soluyanov, Phys. Rev. Lett. **117**(7), 076403 (2016).
[11]Z. M. Zhu, G. W. Winkler, Q. S. Wu, J. Li, and A. A. Soluyanov, Phys. Rev. X **6**(3), 031003 (2016).
[12]J. P. Omaggio, J. R. Meyer, R. J. Wagner, C. A. Hoffman, M. J. Yang, D. H. Chow, and R. H. Miles, Appl. Phys. Lett. **61**(2), 207 (1992).
[13]C. R. Pidgeon, D. L. Mitchell, and R. N. Brown, Phys. Rev. **154**(3), 737 (1967).
[14]J. C. Maan, Y. Guldner, J. P. Vieren, P. Voisin, M. Voos, L. L. Chang, and L. Esaki, Solid State Commun. **39**(5), 683 (1981).
[15]D. H. Lu, I. M. Vishik, M. Yi, Y. L. Chen, R. G. Moore, and Z. X. Shen, Annu. Rev. Condens. Matter Phys. **3**, 129–167 (2012).
[16]I. K. D. Chung Koo Kim, K. Fujita, J. C. Séamus Davis, I. Božović, and T. Valla, e-print arXiv:1805.04811.
[17]I. K. Drozdov, I. Pletikosić, C. K. Kim, K. Fujita, G. D. Gu, J. C. S. Davis, P. D. Johnson, I. Božović, and T. Valla, Nat. Commun. **9**(1), 5210 (2018).
[18]T. Andlauer and P. Vogl, Phys. Rev. B **80**(3), 035304 (2009).
[19]P. T. Webster, N. A. Riordan, S. Liu, E. H. Steenbergen, R. A. Synowicki, Y. H. Zhang, and S. R. Johnson, J. Appl. Phys. **118**(24), 245706 (2015).
[20]S. P. Svensson, W. A. Beck, W. L. Sarney, D. Donetsky, S. Suchalkin, and G. Belenky, Appl. Phys. Lett. **114**(12), 122102 (2019).
[21]N. Olszowska, J. Lis, P. Ciochon, L. Walczak, E. G. Michel, and J. J. Kolodziej, Phys. Rev. B **94**(11), 115305 (2016).
[22]S. Abe, T. Inaoka, and M. Hasegawa, Phys. Rev. B **66**(20), 205309 (2002).
[23]V. Y. Aristov, G. Le Lay, V. M. Zhilin, G. Indlekofer, C. Grupp, A. Taleb-Ibrahimi, and P. Soukiassian, Phys. Rev. B **60**(11), 7752 (1999).
[24]J. Ludwig, Y. B. Vasilyev, N. N. Mikhailov, J. M. Poumirol, Z. Jiang, O. Vafek, and D. Smirnov, Phys. Rev. B **89**(24), 241406 (2014).
[25]B. Laikhtman, S. Suchalkin, G. Belenky, and M. Ermolaev, Superlattices Microstruct. **128**, 438 (2019).
[26]M. Altarelli, Phys. Rev. B **28**(2), 842 (1983).
[27]B.-J. Yang and N. Nagaosa, Nat. Commun. **5**, 4898 (2014).
[28]G. B. Stringfellow and G. S. Chen, J. Vac. Sci. Technol. B **9**(4), 2182 (1991).
[29]Y. A. Bychkov and E. I. Rashba, JETP Lett. **39**(2), 78 (1984).
[30]M. P. Seah and W. A. Dench, Surf. Interface Anal. **1**(1), 2–11 (1979).